Kinetics of Copolymerization of PEG-Containing Multiacrylates with Acrylic Acid

Robert A. Scott and Nicholas A. Peppas*

School of Chemical Engineering, Purdue University, West Lafayette, Indiana 47907-1283

Received April 20, 1998; Revised Manuscript Received July 22, 1999

ABSTRACT: The compositional dependence of the polymerization kinetics of multiacrylate copolymers with acrylic acid (AA) was examined. The multiacrylates considered were di- or triacrylate esters of oligo(ethylene glycol) (OEG). The multiacrylate polymerization rate increased with the OEG chain length in the absence of added AA. This monomer size dependence was due to mobility-related effects on the pendant double-bond reactivity. AA-containing systems exhibited a slight rate enhancement at high conversions, relative to multiacrylate homopolymer formulations, reflecting changes in the fractional concentration of pendant double bonds. These effects were captured in a free volume-based model of the diffusion-controlled polymerization kinetics.

Introduction

Homopolymerization reactions of multifunctional acrylates and methacrylates have long been of interest due to the anomalous polymerization behavior observed[1−5] in these systems and to the wide range of potential applications[6−10] for highly cross-linked polymer glasses. Therefore, there exists a substantial body of knowledge regarding the mechanism and features of multi(meth)acrylate homopolymerizations, as well as regarding the properties and structure of the resulting highly cross-linked materials. However, despite the fact that multi(meth)acrylate copolymerization reactions offer a route to highly cross-linked materials with precisely controlled properties, the kinetics of these reactions have not been carefully considered. In this work, the kinetics of copolymerizations of acrylic acid (AA) with oligo(ethylene glycol) multiacrylates are considered. Copolymerization with AA offers a facile means of precisely modifying the properties of these networks over a wide range. Materials prepared by copolymerization of OEG multiacrylates with AA may also exhibit pH-dependent behavior, including the formation of interchain hydrogen bonds under appropriate pH conditions.

The most prominent feature of bulk polymerization reactions involving multifunctional monomers is the strong influence of diffusional effects arising due to the formation of an infinite network. Much of the pioneering work in characterizing these effects was carried out by Kloosterboer and collaborators.[8,9,11−15] In addition, there have been several systematic investigations of the influence of monomer structure on the kinetics of polymerization for multimethacrylate and multiacrylate systems.[6,16−23]

In bulk cross-linking polymerizations, the viscosity of the reaction medium increases greatly over the course of polymerization (and from the beginning of the reaction), creating a significant diffusional resistance to the bimolecular macroradical termination reaction. As a result, the rate coefficient, k_t, which describes the kinetics of the bimolecular termination reaction, decreases with conversion. The polymerization rate, which scales as $k_t^{-1/2}$, increases even as reactive double bonds are consumed. This autoacceleration of the polymerization rate due to diffusional effects is known as the Trommsdorff or gel effect.[24]

The magnitude and onset conversion of the gel effect have been shown to depend strongly on the monomer structure for various multi(meth)acrylates. The gel effect was shown to be strongest for compact monomers, with minimal spatial separation between reactive double bonds, since these monomers give the most highly cross-linked networks. Scranton et al.[18] demonstrated this monomer size dependence for a series of oligo(ethylene glycol) dimethacrylates, and Anseth et al.[21] subsequently obtained similar results. Maximum polymerization rates were shown to decrease with increasing ethylene glycol spacer length due to increased radical mobility at larger mesh sizes. Anseth et al.[19] used similar mobility arguments to explain their findings regarding the increasing dependence of the magnitude of the gel effect on monomer functionality.

The impact of diffusional considerations on the kinetics of bulk cross-linking homopolymerizations extends well beyond a monomer-dependent gel effect. At sufficiently high double-bond conversions, the glass transition temperature, T_g, of the developing polymer network surpasses the reaction temperature, and vitrification occurs, leading to limiting double-bond conversions.[15] Polymerization proceeds extremely slowly in the vitrified state due to the extremely low diffusivity of free monomer in the glassy polymer matrix. Limiting double-bond conversion values show a similar dependence on chain mobility to that observed for the magnitude of the gel effect.

Vitrification in multi(meth)acrylate polymerizations is a kinetic phenomenon, depending not only on the level of monomer conversion but also on the rate at which the polymerization proceeds. Hence, limiting double-bond conversions may vary for a given multi(meth)acrylate monomer, depending on the reaction conditions. This behavior arises due to a coupling of the polymerization kinetics and the volume relaxation kinetics. Excess free volume develops during polymerization due to the impact of an infinite network structure on the polymer chain dynamics. The volume relaxation kinetics are substantially slower than the polymerization kinetics,[11] and the system volume is positively displaced from

10.1021/ma9806110 CCC: $18.00
Published on Web 08/25/1999

equilibrium at all times. When the reaction rate is very fast, more double bonds are able to react during the time in which the network chains relax to their equilibrium volume, leading to increased vitrification-limited double-bond conversions.[14] Experimentally, a strong initiation rate dependence (light intensity dependence for photopolymerization) of the limiting double-bond conversion was observed for multiacrylate bulk polymerizations.[6] Additionally, the rate and extent of volume shrinkage were shown to depend strongly on monomer structure.[16,21,25]

Vitrification may also lead to radical trapping. The existence of trapped radicals in photopolymerized poly(multiacrylates) may lead to additional reaction when a thermal after-cure is applied[11] and has been interpreted as an indication of structural heterogeneity. Radicals become trapped in highly cross-linked microgel regions which exist in a less densely cross-linked polymer matrix.[12]

The time-evolving network structure of polymultiacrylates is characterized by pendant double bonds, formed when one of the double bonds on a free monomer molecule reacts into the polymer network. Pendant double bonds are tethered to the network backbone and, therefore, are substantially less mobile than free double bonds. Measurements of the conversion-dependent cross-linking density over the course of multiacrylate polymerizations[9] indicated that, during the early stages of polymerization, pendant double bonds are consumed preferentially due to their locally high concentration. However, near the end of the polymerization, free double bonds exhibit a higher apparent reactivity. Additionally, cyclization reactions between radicals and double bonds pendant to the radical-bearing chain were shown to contribute significantly to structural development during polymerization.[26,27]

Efforts to model multi(meth)acrylate polymerizations have relied heavily on free volume approaches. Bowman and Peppas[28] coupled free volume-derived expressions for diffusion-controlled k_p and k_t values to expressions describing the time-dependent evolution of the system free volume in order to predict multimethacrylate homopolymerization behavior using three adjustable parameters. This model was later expanded by Anseth et al.[29] to accommodate termination based on "reaction diffusion," a mechanism by which radicals move toward one another by propagating through double bonds in the intervening space.

Kurdikar and Peppas[30] used the Vrentas−Duda[31,32] free volume theory of diffusion and the Smoluchowski[33] expression for diffusion-controlled reaction rate coefficients to develop a first-principles approach for describing multiacrylate polymerization behavior. This model also accounted for the finite rate of volume relaxation and additionally allowed for diffusional effects on the initiator efficiency. Both the Bowman−Peppas and the Kurdikar−Peppas approaches relied on the assumption that pendant and free double bonds react with equal probability over the entire course of the polymerization.

We have recently examined the structure and properties of a new class of materials prepared by copolymerization techniques, using AA and various poly(ethylene glycol)-containing multiacrylates. The material characteristics were shown to vary over a wide range, depending on the AA and poly(ethylene glycol) (PEG) contents. In the present work, the compositional dependence of the photopolymerization kinetics is examined for various AA−multiacrylate systems. The experiments were designed to elucidate the effects for multiacrylate monomers having various PEG chain lengths of diluting the pool of reactive double bonds with difunctional AA monomer. Compositional effects on the polymerization rate curves and on the limiting double-bond conversions were measured and examined in terms of free volume theory.

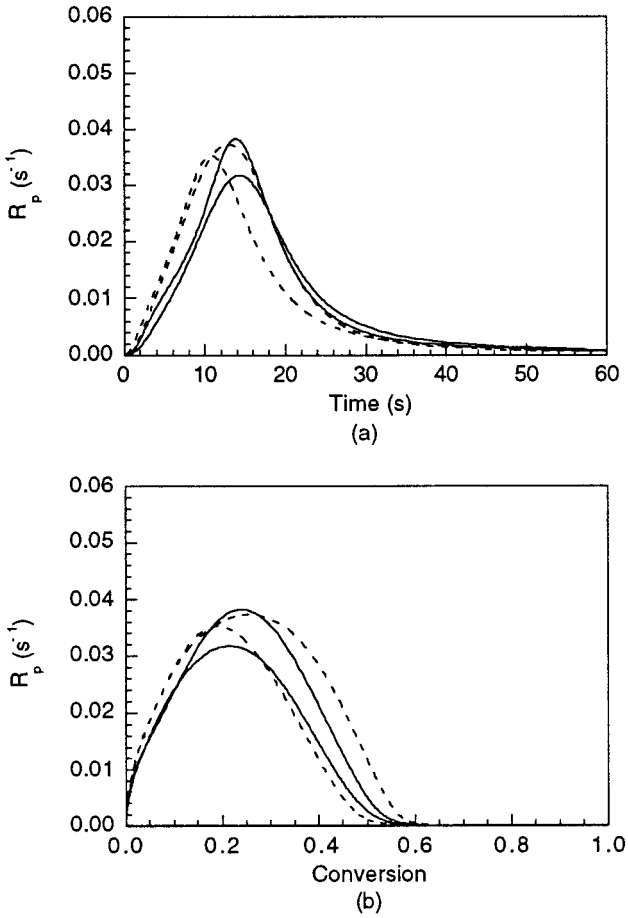

Figure 1. Polymerization rate, R_p, as a function of time (a) and as a function of conversion (b) for systems D2 (—) and D2−25 (- - -). Solutions contained 1 wt % DMPA and were polymerized at 30 °C under a N_2 purge using 0.1 mW/cm^2 of incident UV radiation.

Experimental Section

Materials. The various monomers used in the preparation of copolymer networks are shown in Figure 1 of the preceding paper. The diacrylates were ethylene glycol diacrylate (EGDA, $n = 1$), di(ethylene glycol) diacrylate (DEGDA, $n = 2$), tri(ethylene glycol) diacrylate (TrEGDA, $n = 3$), poly(ethylene glycol) (MW = 200) diacrylate (PEG200DA, $n \approx 4$), and poly(ethylene glycol) (MW = 400) diacrylate (PEG400DA, $n \approx 9$) (Polysciences, Warrington, PA). The triacrylates were trimethylolpropane triacrylate (TrMPTrA, Polysciences) and a series of ethoxylated analogues (Aldrich, Milwaukee, WI) of TrMPTrA. The analogues contained 3 (PEG170TrA), 7 (PEG290TrA), and 14 (PEG500TrA) ethoxy groups per monomeric unit. The multiacrylate monomers were used as received, without further purification. The nominal molecular weights are therefore average values, and impurities with molecular weights greater than or less than the average value will contribute to the network structure of polymers prepared from these monomers.

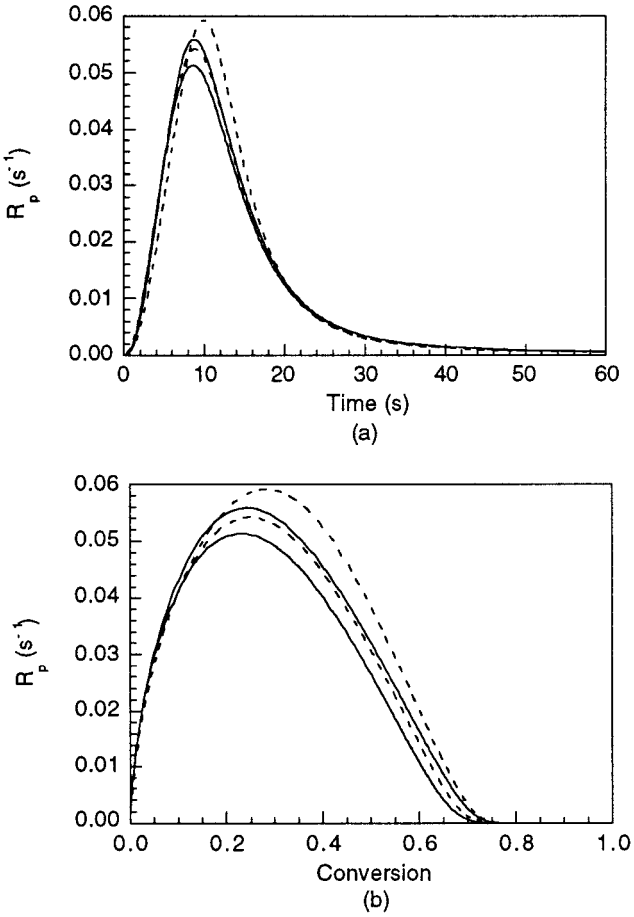

Figure 2. Polymerization rate, R_p, as a function of time (a) and as a function of conversion (b) for systems D4 (—) and D4—30 (- - -). Solutions contained 1 wt % DMPA and were polymerized at 30 °C under a N_2 purge using 0.1 mW/cm^2 of incident UV radiation.

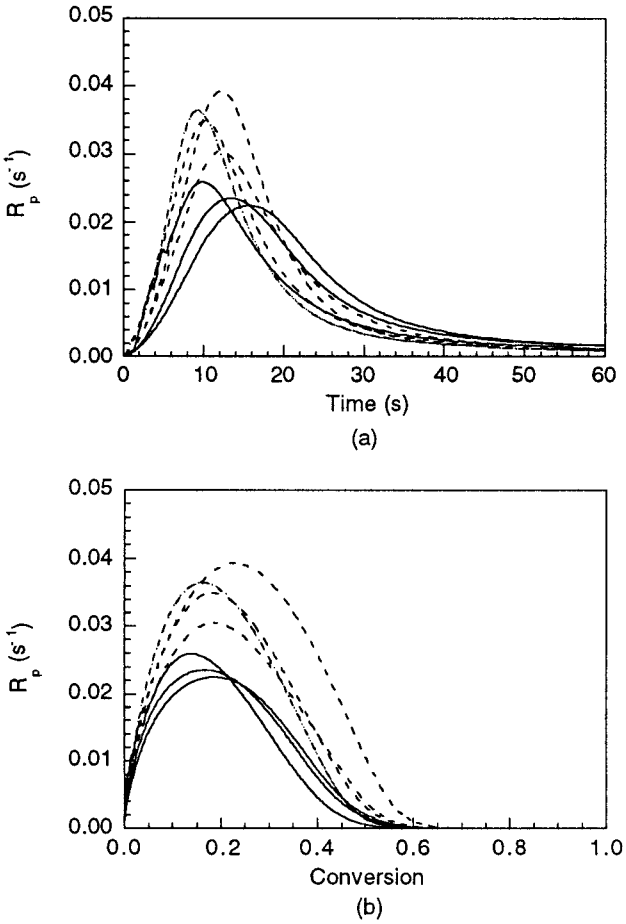

Figure 3. Polymerization rate, R_p, as a function of time (a) and as a function of conversion (b) for systems T3 (—) and T3-30 (- - -). Solutions contained 1 wt % DMPA and were polymerized at 30 °C under a N_2 purge using 0.1 mW/cm^2 of incident UV radiation.

The AA molar feed content in multiacrylate copolymers was varied from 0 to 40 mol %, based on double bonds. A code name beginning with D (for diacrylates) or T (for triacrylates) was used to uniquely identify each copolymer according to PEG chain length and AA content. For example, D2-40 was used to indicate poly(DEGDA-*co*-40% AA).

Monomer mixtures were prepared by mixing distilled AA (Aldrich) and a multiacrylate monomer in appropriate quantities. A typical formulation contained 40 mol % AA and 60 mol % PEG200DA, with photoinitiator 2,2-dimethoxy-2-phenylacetophenone (DMPA, Aldrich) added at a concentration of 1 wt %, based on total monomer weight.

Methods. The polymerization kinetics of the various formulations were studied using differential scanning photocalorimetry (DPC). Experiments were performed under a N_2 purge on a differential scanning photocalorimeter (model DPC 930, TA Instruments, New Castle, DE). Samples having a mass of approximately 2.0 mg were polymerized in aluminum sample pans under 0.1 mW/cm^2 of incident UV irradiation. The UV light source was a 200 W mercury arc lamp with maximum intensity at 365 nm, and the light intensity was controlled using neutral density filters (Melles Griot, Boulder, CO). All monomer samples were covered with a thin polyethylene film in order to minimize loss of monomer due to evaporation. In all cases, the measured change in mass at the end of cure was less than 1 wt %. An empty aluminum sample pan with polyethylene cover was used as a heat flow reference for all experiments.

Theoretical reaction enthalpies were calculated for each formulation using the known enthalpies of 18.5 kcal/mol for AA double bonds[34] and 20.6 kcal/mol for acrylate double bonds.[1] The latter value is that measured for lauryl acrylate.[1] Hence, the polymerization rate, R_p, in units of fractional double-bond conversion per second, was calculated by dividing the measured heat flow per unit mass at any given time by the calculated theoretical reaction enthalpy. The time-dependent double-bond conversion was calculated by numerical integration of the rate data.

Results and Discussion

Compositional Effects on Photopolymerization Kinetics. Figures 1—4 show representative rate curves for various di- and triacrylate formulations polymerized using a light intensity of 0.1 mW/cm^2. Part a of each figure depicts the time dependence of R_p, while part b depicts the conversion dependence. Each plot shows multiple measurements of the polymerization rate for a multiacrylate homopolymer system and for a system with 20—40 mol % of added AA.

Figures 1—4 show that R_p increased with the PEG chain length for diacrylate and triacrylate systems. Also, the figures show that, qualitatively, the effects of added AA on the photopolymerization kinetics of multiacrylate systems were very different for diacrylate monomers (Figures 1 and 2) than for triacrylate monomers (Figures 3 and 4). Rate curves measured for the diacrylate copolymers with AA were very similar in shape to those measured for the diacrylate homopolymers. Differences due to added AA were on the order of the reproducibility limits of the experiments, although the results for

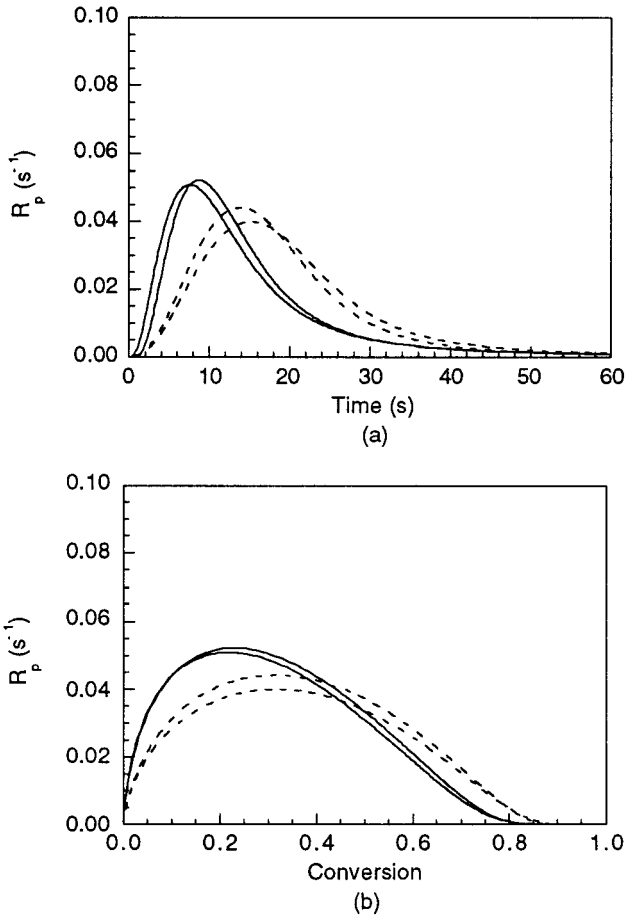

Figure 4. Polymerization rate, R_p, as a function of time (a) and as a function of conversion (b) for systems T10 (—) and T10-35 (- - -). Solutions contained 1 wt % DMPA and were polymerized at 30 °C under a N_2 purge using 0.1 mW/cm^2 of incident UV radiation.

several systems indicated that copolymerization with AA led to a slight enhancement of R_p near the end of the polymerization. This trend reflects the reduced contribution of pendant double bonds to the overall reactivity near the end of the reaction in the presence of AA.

The effects of added AA on the copolymerization kinetics were significantly stronger for the triacrylate systems. Figure 3 shows that R_p for the T3-30 system was substantially higher over the course of the polymerization than R_p for the T3 homopolymer system. However, Figure 4 shows that copolymerization with AA led to a reduction in R_p for the T10 system, with the longest PEG chains. Clearly, the dependence of R_p on the AA content was coupled to the PEG chain length dependence of the kinetics.

Each rate curve was characterized by a maximum value of the polymerization rate, $R_{p,max}$, whose magnitude and position along the conversion axis varied with the structure of the multiacrylate monomer. Measured values of $R_{p,max}$ are provided in Table 1, along with measured values of the initial polymerization rate, $R_{p,i}$, measured at 5% conversion. Additionally, the table shows the conversion, p_{max}, corresponding to $R_{p,max}$, and the final double-bond conversion, p_∞.

Table 1 illustrates several important trends regarding the compositional dependence of the photopolymerization kinetics of multiacrylate−AA systems. First of all, $R_{p,i}$ and $R_{p,max}$ clearly increased with the PEG chain length. This trend reflects the chain length dependence of the pendant double-bond reactivity. As the length of the PEG "tether" which binds the pendant double bond to the network backbone increased, the mobility, and hence the reactivity, of the pendant double bond increased. The fact that this effect was monitored by both $R_{p,i}$ and $R_{p,max}$ indicates that mobility considerations

Table 1. Measured Kinetic Parameters for AA/ Multiacrylate Copolymerizations, with 95% Confidence Limits[a]

composition	$R_{p,i}$ (±0.003 s^{-1})	$R_{p,max}$ (±0.005 s^{-1})	p_{max} (±0.03)	p_∞ (±0.06)
D1	0.022	0.030	0.13	0.53
D1-20	0.024	0.036	0.15	0.57
D2	0.016	0.035	0.23	0.61
D2-25	0.019	0.036	0.23	0.61
D3	0.025	0.046	0.22	0.71
D3-30	0.022	0.049	0.25	0.68
D4	0.030	0.054	0.24	0.75
D4-30	0.028	0.057	0.27	0.77
D9	0.034	0.056	0.26	0.96
D9-30	0.031	0.059	0.30	0.95
T3	0.016	0.024	0.16	0.62
T3-30	0.020	0.035	0.19	0.67
T6	0.030	0.042	0.17	0.71
T6-35	0.030	0.052	0.24	0.74
T10	0.033	0.052	0.22	0.89
T10-35	0.021	0.042	0.31	0.93

[a] Polymerizations were performed at 30 °C under an N_2 purge, using 1 wt % DMPA photoinitiator and 0.1 mW/cm^2 of incident UV light intensity.

Table 2. Compositional Parameters of Various Multiacrylate−AA Formulations, Used in the Free Volume Model of the Copolymerization Kinetics

composition	$f/2$	$[M_1]_0$ (mol/L)	$[M_2]_0$ (mol/L)	$w_{1,0}$
D1	2		13.06	
D1-20	2	4.05	9.44	0.267
D2	2		10.37	
D2-25	2	3.41	7.95	0.224
D3	2		8.61	
D3-30	2	2.94	6.87	0.193
D4	2		6.81	
D4-30	2	2.43	5.68	0.159
D9	2		4.22	
D9-30	2	1.61	3.76	0.105
T3	3		7.78	
T3-30	3	2.71	6.33	0.178
T6	3		5.51	
T6-35	3	2.03	4.75	0.133
T10	3		3.65	
T10-35	3	1.41	3.30	0.092

Table 3. Free Volume Model Parameters for Various Multiacrylate−AA Formulations

composition	$\hat{V}_2$* (cm^3/g)	r_{m2} (Å)	T_{g3} (°C)	α
D1	0.42	3.1	61	0.45
D1-20			150	0.45
D2	0.49	3.4	118	1.0
D2-25			115	1.0
D3	0.54	3.6	65	2.0
D3-30			79	2.0
D4	0.60	3.9	47	4.5
D4-30			68	4.5
D9	0.67	4.5	−12	7.5
D9-30			12	7.5
T3	0.57	4.2	108	1.0
T3-30			131	1.0
T6	0.66	4.8	39	4.7
T6-35			59	4.7
T10	0.71	5.5	−8	9.1
T10-35			18	9.1

dominate the polymerization kinetics from the beginning of the reaction. The conversion parameters p_{max} and p_∞ also increased with increasing PEG chain length, again reflecting effects on the pendant double-bond reactivity. A very substantial increase in p_{max} was observed between the D1 and D2 systems, indicating that the pendant double bonds in the D1 system were extremely constrained.

The kinetic parameters in Table 1 also show quantitatively that the triacrylate polymerization kinetics were substantially more sensitive to the effects of added AA than were the diacrylate polymerization kinetics. This effect of the monomer functionality reflects the difference in pendant double concentrations for polydiacrylates and polytriacrylates. Because each addition of free triacrylate monomer to the growing polymer network leads to the formation of two pendant double bonds (versus one pendant double bond for the diacrylate monomer), the contribution of the pendant double-bond reactivity to the overall polymerization kinetics is more heavily weighted for triacrylates than for diacrylates. In this context, copolymerization with AA affects the polymerization kinetics by altering the fractional population levels of various double-bond types, and the measured effects of added AA on the triacrylate polymerization kinetics reflect the diminished contribution of the pendant double-bond reactivity to the overall polymerization kinetics. The pendant double-bond reactivity for the T3 system was relatively small due to mobility effects, and copolymerization with AA led to an increase in R_p. However, the pendant double-bond reactivity for the T10 system was relatively large, and copolymerization with AA led to a decrease in R_p.

The calorimetric experiments clearly show that the compositional dependence of the polymerization kinetics for multiacrylate systems is mediated by the relative contributions of free and pendant double bonds to the overall reactivity of the system. Therefore, the effects of copolymerization with AA are based on the resulting changes in the relative concentrations of free and pendant double bonds. As the structure of the multiacrylate monomer is varied, these copolymerization effects are superimposed upon monomer size−reactivity effects.

Free Volume Model of Copolymerization Kinetics. Free volume-based models are well-suited for the description of polymerization processes dominated by diffusional considerations, such as bulk cross-linking polymerizations. Therefore, a free volume approach was pursued in order to describe the measured compositional dependence of the multiacrylate−AA copolymerization kinetics.

Kurdikar and Peppas[30,35] developed a model to describe the diffusion-controlled bulk polymerization kinetics of DEGDA. This model was based on the Smoluchowski theory[33] of diffusion-controlled reactions. Rate coefficients k_p and k_t, for radical propagation and bimolecular radical termination, respectively, were calculated over the course of the reaction on the basis of monomer and radical diffusivities:[30]

$$k_{p,trans} = 4\pi(r_m + r_r)D_{m,trans} \quad (1)$$

$$k_t = 4\pi(r_m + r_r)D_{rp} \quad (2)$$

Here, $k_{p,trans}$ is the propagation rate coefficient based on the translational diffusion characteristics of the monomer, described by the translational diffusion coefficient, $D_{m,trans}$. The overall propagation rate coefficient, k_p, contained an additional contribution due to segmental diffusion effects. The parameter D_{rp} is the effective diffusion coefficient of the radical, based on a reaction diffusion mechanism for radical motion.[30] The terms r_m and r_r are the Lennard-Jones radii of the monomer and the radical, respectively.

The conversion dependence of the polymerization rate coefficients was described by the parameter $D_{m,trans}$. Diffusion coefficient values were calculated over the course of the polymerization according to the Vrentas−Vrentas[36] modification of the Vrentas−Duda[31,32] diffusion theory:

$$D_{m,trans} = D_0 \exp\left(-\frac{E}{RT}\right)\exp\left[-\frac{\gamma(w_1\hat{V}_1^* + \xi w_2\hat{V}_2^*)}{\hat{V}_{FH}}\right] \quad (3)$$

Here, D_0 is a constant preexponential factor, E is the activation energy for a diffusional jump, R is the gas constant, and T is the system temperature. The second exponential term describes the free volume dependence of the monomer diffusion coefficient. The parameters w_1 and w_2 are the weight fractions of monomer and polymer, respectively, at any given time over the course of the polymerization. The terms $\hat{V}_1^*$ and $\hat{V}_2^*$ are the critical specific hole volumes required for a diffusional jump of the monomer or polymer, and $\hat{V}_{FH}$ is the conversion-dependent specific hole free volume of the polymerizing system. Volume relaxation effects are captured by $\hat{V}_{FH}$. The parameter γ accounts for free volume overlap, and ξ describes the ratio of the molar volume of the monomer jumping unit to that of the polymer jumping unit.

The diffusion-controlled rate coefficients k_p and k_t were used to calculate the double-bond and radical concentrations, [M] and [M$^\bullet$], using the following differential equations:

$$\frac{d[M]}{dt} = -k_p[M][M^\bullet] \quad (4)$$

$$\frac{d[M^\bullet]}{dt} = R_i - 2k_t[M^\bullet]^2 \quad (5)$$

The term R_i is the rate of initiation, which depends on the polymerization conditions. The double-bond concentration, [M], includes free double bonds on unreacted monomer molecules, as well as double bonds pendant to the polymer network backbone. The reactivity of these double bonds is described by a single rate coefficient, k_p.

Using parameters appropriate for the DEGDA system, Kurdikar and Peppas[30] showed that the polymerization kinetics of that system were well-described by such a treatment. However, extension of this treatment to multiacrylate−AA copolymer systems required that two important issues were addressed: (i) how to account for the increasing dependence of the polymerization rate on the PEG chain length, observed for the homopolymerization of PEG-containing multiacrylates, and (ii) how to account for the diffusional implications of the addition of the more compact AA monomer to the polymerizing system.

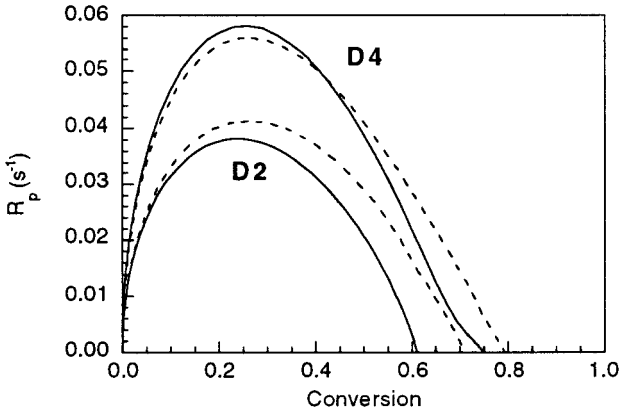

Figure 5. Model-predicted rate curves for systems D2 and D4 (—) and for systems D2-25 and D4-30 (- - -), illustrating the free volume-derived effects of varying the PEG chain length and the AA content for polymerizing systems. Reaction conditions were 30 °C with a UV light intensity of 0.1 mW/cm^2.

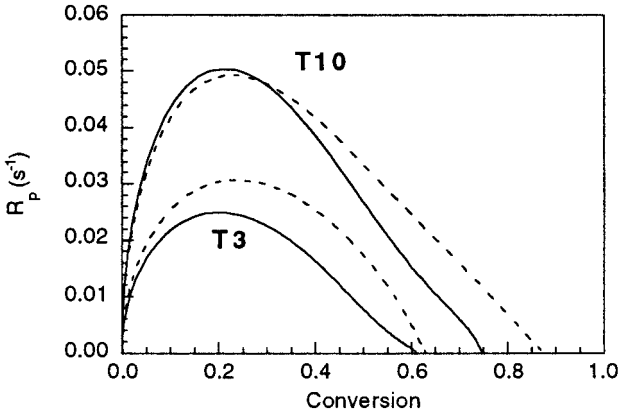

Figure 6. Model-predicted rate curves for systems T3 and T10 (—) and for systems T3-30 and T10-35 (- - -), illustrating the free volume-derived effects of varying the PEG chain length and the AA content for polymerizing systems. Reaction conditions were 30 °C with a UV light intensity of 0.1 mW/cm^2.

To address these issues, eq 3 was modified to accommodate two monomeric species competing for diffusional free volume:

$$D_{m1,trans} = D_0 \exp\left(-\frac{E}{RT}\right) \times \exp\left[-\frac{\gamma(w_1\hat{V}_1^* + (\xi_1/\xi_2)w_2\hat{V}_2^* + \xi_1 w_3\hat{V}_3^*)}{\hat{V}_{FH}}\right] \quad (6)$$

$$D_{m2,trans} = D_0 \exp\left(-\frac{E}{RT}\right) \times \exp\left[-\frac{\gamma((\xi_2/\xi_1)w_1\hat{V}_1^* + w_2\hat{V}_2^* + \xi_2 w_3\hat{V}_3^*)}{\hat{V}_{FH}}\right] \quad (7)$$

Here, $D_{m1,trans}$ is the diffusion coefficient of AA and $D_{m2,trans}$ is the diffusion coefficient of the multiacrylate monomer. On the right-hand side of eqs 6 and 7, the subscripts 1, 2, and 3 indicate parameters for AA, the multiacrylate monomer, and the polymer, respectively. The monomer-specific parameters are the critical specific hole volumes for diffusional displacement, $\hat{V}_1^*$ and $\hat{V}_2^*$, and the jumping unit molar volume ratios, ξ_1 and ξ_2. The parameter ξ_1 is the ratio of the molar volume of the AA jumping unit to that of the polymer jumping unit, and ξ_2 is the ratio of the molar volume of the multiacrylate jumping unit to that of the polymer jumping unit.

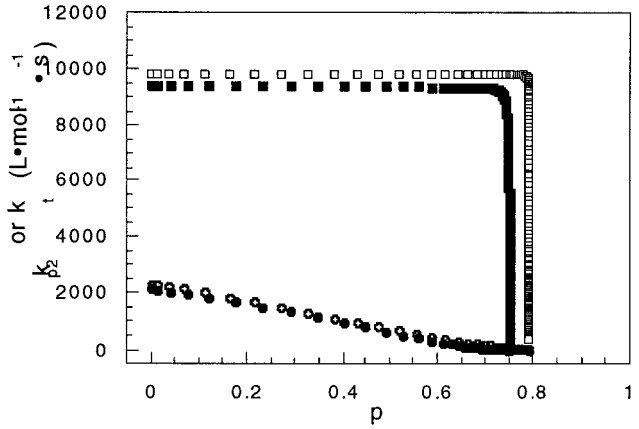

Figure 7. Predicted conversion-dependent rate coefficients for D4 and D4-30 systems: ■, k_{p2} (D4); □, k_{p2} (D4-30); ●, k_t (D4); ○, k_t (D4-30).

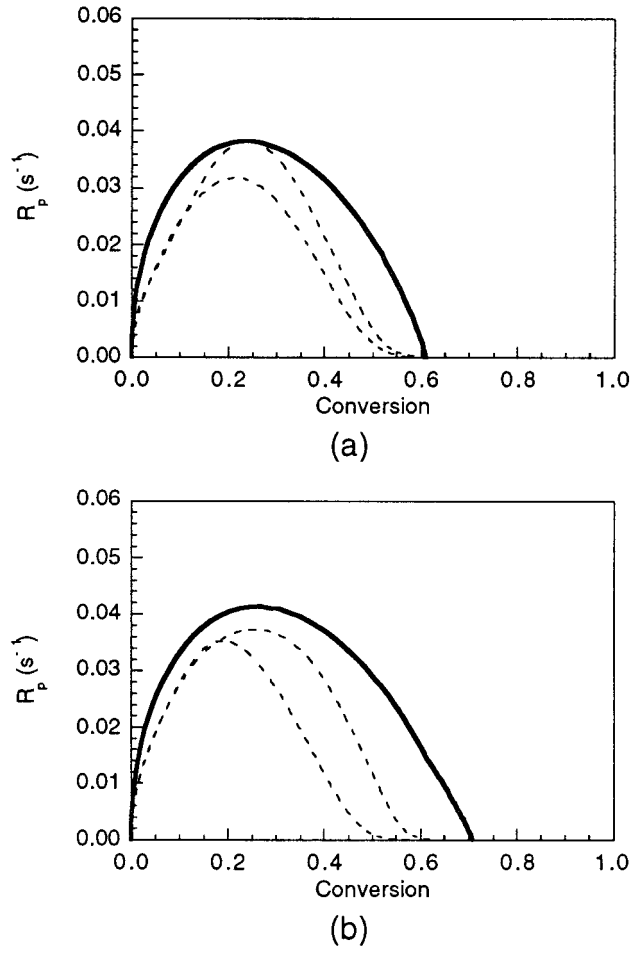

Figure 8. Comparison of experimental (- - -) and predicted (—) rate curves describing the photopolymerization of systems D2 (a) and D2-25 (b). Reaction conditions were 30 °C with a UV light intensity of 0.1 mW/cm^2.

To implement these equations, group contribution methods[37] were used for the calculation of $\hat{V}_1^*$ and $\hat{V}_2^*$ for the various multiacrylate−AA formulations. The terms ξ_1 and ξ_2 were calculated using the following equations:

$$\xi_1 = \frac{\hat{V}_1^* M_1}{0.6224 T_{g3}(\mathrm{K}) - 86.95} \tag{8}$$

$$\xi_2 = \xi_1 \frac{\hat{V}_2^*}{\hat{V}_1^*} \tag{9}$$

Here, M_1 is the molecular weight of AA. The denominator of eq 8 represents an empirical expression[37] describing the dependence of the molar volume of the polymer jumping unit on the polymer glass transition temperature, T_{g3}. Values of T_{g3} for the fully cured ($p = p_\infty$) polymer systems were available from dynamic mechanical analysis experiments. Clearly, the use of a single T_{g3} value for each system limits the ability of the model to accurately predict the kinetics over the entire range of conversions. However, this approach should capture effects of varying the monomer structure on the polymerization kinetics.

Equation 9 represents the critical assumption that the diffusion of the bulky multiacrylate monomer in the cross-linked polymer matrix does not require motion of the entire molecule. Rather, the diffusional process is characterized by a jumping unit whose molecular weight is on the order of that of AA.

In the modified model, the rates of consumption of AA double bonds and free multiacrylate double bonds were described separately:

$$\frac{d[M_1]}{dt} = -k_{p1}[M_1][M^\bullet] \tag{10}$$

$$\frac{d[M_2]}{dt} = -\frac{f}{2}k_{p2}[M_2][M^\bullet] \tag{11}$$

Propagation rate coefficients for AA double bonds and free multiacrylate double bonds, k_{p1} and k_{p2}, were calculated from $D_{m1,trans}$ and $D_{m2,trans}$, as described above. The term $f/2$ in eq 11 is the number of double bonds per multiacrylate molecule and accounts for the fact that when a free double bond on a multiacrylate monomer molecule reacts, the other double bonds on that monomer molecule become pendant to the network backbone. The concentration of pendant double bonds was followed separately:

$$\frac{d[M_p]}{dt} = \left\{\left(\frac{f}{2} - 1\right)k_{p2}[M_2] - k_{pp}[M_p]\right\}[M^\bullet] \tag{12}$$

The terms k_{pp} and $[M_p]$ are the rate coefficient for propagation through pendant double bonds and the pendant double-bond concentration, respectively.

Equations 5 and 10−12 are sufficient to describe the polymerization process, with all of the necessary rate coefficients except for k_{pp} determined according to eqs 1, 2, 6, and 7. To determine k_{pp} over the course of the polymerization, it was assumed that the free double-bond and pendant double-bond reactivities were initially equal ($k_{p2} = k_{pp}$, $p = 0$) and that pendant double bonds were trapped upon vitrification ($k_{pp} = 0$, $p = p_\infty$). As an initial approximation, k_{pp} was allowed to vary linearly over the range $p = 0$ to $p = p_\infty$, where p is the double-bond conversion:

$$k_{pp} = \left(1 - \frac{p}{p_\infty}\right)k_{p2} \tag{13}$$

Table 4. Measured Kinetic Parameters for AA/ Multiacrylate Copolymerizations, with 95% Confidence Limits, Compared with Free Volume Model Predictions[a]

	$R_{p,i}$ (s^{-1})		R_{pmax} (s^{-1})		p_{max}	
composition	expt (±0.003)	model	expt (±0.005)	model	expt (±0.03)	model
D2	0.016	0.023	0.035	0.038	0.23	0.23
D2-25	0.019	0.025	0.036	0.041	0.23	0.27
D4	0.030	0.037	0.054	0.058	0.24	0.26
D4-30	0.028	0.035	0.057	0.056	0.27	0.27
T3	0.016	0.017	0.024	0.025	0.16	0.20
T3-30	0.020	0.019	0.035	0.031	0.19	0.24
T10	0.033	0.034	0.052	0.050	0.22	0.21
T10-35	0.021	0.031	0.042	0.049	0.31	0.22

[a] Polymerizations were performed at 30 °C under an N_2 purge, using 1 wt % DMPA photoinitiator and 0.1 mW/cm^2 of incident UV light intensity.

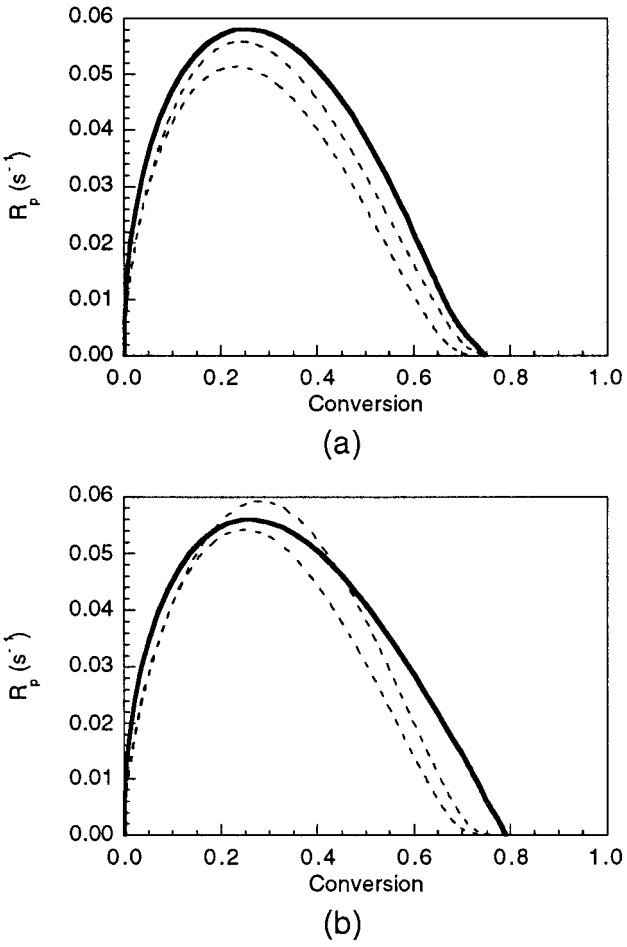

Figure 9. Comparison of experimental (- - -) and predicted (—) rate curves describing the photopolymerization of systems D4 (a) and D4-30 (b). Reaction conditions were 30 °C with a UV light intensity of 0.1 mW/cm^2.

This description gives a substantially stronger conversion dependence for k_{pp} than that predicted for k_{p2} on the basis of diffusional considerations. This behavior is reasonable due to the reduction in mobility expected for pendant double bonds upon attachment to the network.

Tables 2 and 3 provide a listing of the composition-dependent model parameters, used in the calculations described above. Additionally, group contribution methods were used to calculate a $\hat{V}_1^*$ value of 0.45 cm^3/g. Experimental values of p_∞, from Table 1, were also used in the model. For all parameters not listed in the tables,

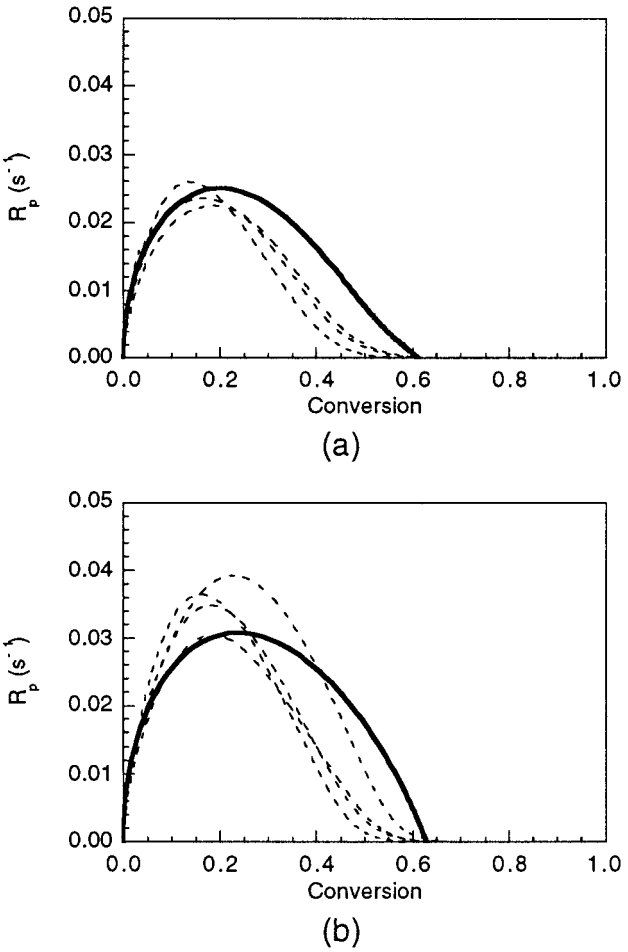

Figure 10. Comparison of experimental (- - -) and predicted (—) rate curves describing the photopolymerization of systems T3 (a) and T3-30 (b). Reaction conditions were 30 °C with a UV light intensity of 0.1 mW/cm^2.

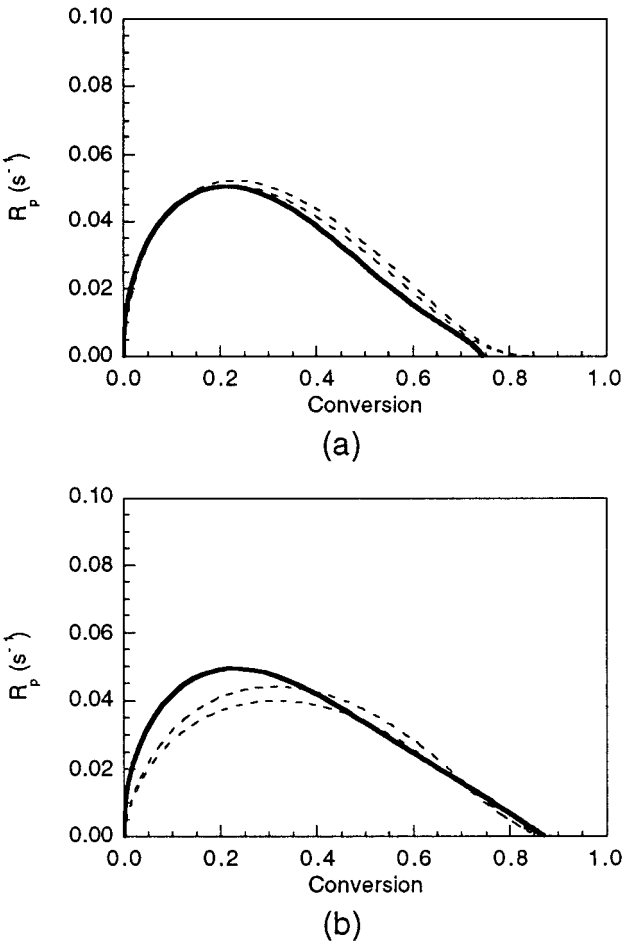

Figure 11. Comparison of experimental (- - -) and predicted (—) rate curves describing the photopolymerization of systems T10 (a) and T10-35 (b). Reaction conditions were 30 °C with a UV light intensity of 0.1 mW/cm^2.

the values reported by Kurdikar and Peppas[30] were used.

The predicted purely diffusion-controlled polymerization rate decreased with increasing size of the multiacrylate monomer, i.e., on the PEG chain length. This behavior was opposite to that observed experimentally, and therefore, an empirical monomer size adjustment parameter, α, was added to the model. Model data for homopolymer systems were matched to experimental data by multiplying the reaction radius term in eq 1 by α. As seen in the Table 3, this adjustment was not necessary for the shortest PEG chain lengths, and the magnitude of the adjustment increased as the PEG chain length increased. The failure of the model in the absence of this additional parameter indicates inaccuracy in the estimation of the reaction radius as the sum of the Lennard-Jones radii of the reacting species. However, once α and p_∞ values were obtained using experimental data for homopolymer systems, the copolymerization kinetics of AA-containing systems were well-described by the model.

Figure 5 shows the predicted compositional dependence of the polymerization rate for D2 and D4 homo- and copolymer systems, polymerized at 30 °C with a UV light intensity of 0.1 mW/cm^2. Figure 6 shows the model predictions for the T3 and T10 systems under the same reaction conditions. The predicted compositional dependence of the polymerization rate is in good agreement with the experimental data in Figures 1−4. Measured and predicted values of various kinetic parameters are compared in Table 4, while Figure 7 shows a typical plot of the model-predicted values of k_{p2} and k_t for a diacrylate system. Theoretical and experimental rate curves are compared directly in Figures 8−11.

The figures and the table clearly show good agreement between experiments and the model regarding the compositional dependence of the polymerization kinetics. However, the model rate curves also exhibit effects that may have been beyond the experimental detection limits. Figures 5 and 6 show that an enhancement of R_p was predicted for AA-containing systems and that the conversion at which this enhancement was observed increased as the PEG chain length was increased. This behavior was observed experimentally for the T3 and T10 systems (Figures 3 and 4) but was obscured in the experimental results for the D2 and D4 systems (Figures 1 and 2).

Figure 6 shows that the model very effectively captured the strong coupling of PEG chain length effects to copolymerization effects for the triacrylate systems. A significant enhancement of R_p for the T3-30 system relative to R_p for the T3 homopolymer system was predicted at all conversions, consistent with experiment. For the T10 system, the R_p enhancement due to added AA was observed only at high conversions. Additionally, the model accurately predicted the existence of an intersection of the T10 and T10-35 rate curves at intermediate conversions.

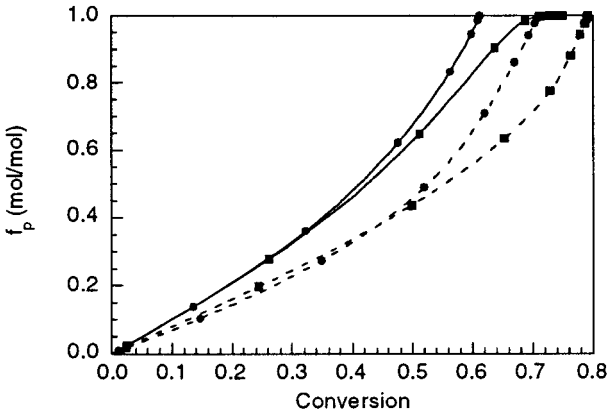

Figure 12. Model-predicted values of the fractional concentration of pendant double bonds, f_p, as a function of conversion for systems D2 (—●—), D4 (—■—), D2-25 (- -●- -), and D4-30 (- -■- -). Reaction conditions were 30 °C with a UV light intensity of 0.1 mW/cm^2.

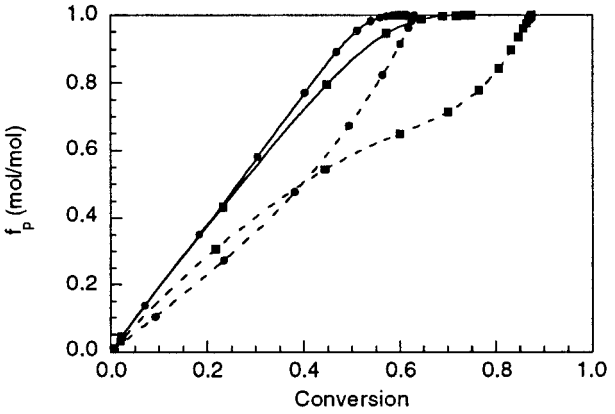

Figure 13. Model-predicted values of the fractional concentration of pendant double bonds, f_p, as a function of conversion for systems T3 (—●—), T10 (—■—), T3-30 (- -●- -), and T10-35 (- -■- -). Reaction conditions were 30 °C with a UV light intensity of 0.1 mW/cm^2.

To examine more carefully this coupling of PEG chain length effects and copolymerization effects, predicted values of the fractional concentration of pendant double bonds, f_p, were calculated as a function of conversion. The results are shown in Figure 12 for diacrylates and in Figure 13 for triacrylates. The data clearly show that the enhancement in R_p observed for AA-containing systems was due to a decrease in f_p at all conversions for the copolymer systems. This decrease in f_p led to a decreased contribution of the immobile pendant double bonds to the overall reactivity of the system.

Additionally, Figures 12 and 13 show that there was a significant chain length dependence of f_p at high conversions for the AA-containing systems. At similar conversions near the end of the polymerization, f_p was less for systems D4-30 and T10-35 than for systems D2-25 and T3-30, respectively. Due to the size dependence of the multiacrylate monomer reactivity, the rate of incorporation of AA into the polymer network decreased with increasing PEG chain length. Therefore, the unreacted AA content was higher at elevated conversions for systems with longer PEG chain lengths, and f_p was lower. This phenomenon led to the intersection of the rate curves for systems T10 and T-35 and for systems D4 and D4-30.

Conclusions

The compositional dependence of the copolymerization kinetics of PEG-containing multiacrylates with AA was considered. The polymerization rate was found to increase with increasing PEG chain length at any given AA concentration. The effects on the polymerization kinetics of varying the AA content were coupled to the PEG chain length dependence and depended very strongly on the multiacrylate functionality. These findings reflected effects of varying the AA content on the contribution of the pendant double-bond reactivity to the overall polymerization kinetics.

A free volume model of the multiacrylate−AA polymerization kinetics was developed. This model computed the rate behavior based on independent rate coefficients describing the reactivities of free and pendant double bonds. Model predictions of PEG chain length effects and AA concentration effects on the copolymerization kinetics were in good agreement with experiment.

Acknowledgment. This work was supported by grants from the National Science Foundation and the National Institutes of Health.

References and Notes

(1) Moore, J. E. In *Chemistry and Properties of Crosslinked Polymers*; Labana, S. S., Ed.; Academic Press: New York, 1977; pp 535−546.
(2) Tyson, G. R.; Shultz, A. R. *J. Polym. Sci., Polym. Phys. Ed.* **1979**, *17*, 2059−2075.
(3) Hubca, G. H.; Oprescu, C. R.; Drăgan, G. H.; Dimonie, M. *Rev. Roumaine Chim.* **1982**, *27*, 433−442.
(4) Drăgan, G. H.; Hubca, G. H.; Oprescu, C. R.; Dimonie, M. *Rev. Roumaine Chim.* **1982**, *27*, 585−590.
(5) Miyazaki, K.; Takashi, H. *J. Biomed. Mater. Res.* **1988**, *22*, 1011−1022.
(6) Kurdikar, D. L.; Peppas, N. A. *Polymer* **1994,** *35*, 1004−1011.
(7) Kurdikar, D. L.; Peppas, N. A. *Polymer* **1995**, *36*, 2249−2255.
(8) Kloosterboer, J. G.; Lijten, G. F. C. M. *Polymer* **1987**, *28*, 1149−1155.
(9) Kloosterboer, J. G.; Lijten, G. F. C. M.; Boots, H. M. J. *Makromol. Chem., Macromol. Symp.* **1989**, *24*, 223−230.
(10) Gossink, R. G. *Angew. Makromol. Chem.* **1986**, *145/146*, 365−389.
(11) Kloosterboer, J. G.; van de Hei, G. M. M.; Gossink, R. G.; Dortant, G. C. M. *Polym. Commun.* **1984**, *25*, 322−325.
(12) Kloosterboer, J. G.; van de Hei, G. M. M.; Boots, H. M. J. *Polym. Commun.* **1984**, *25*, 354−357.
(13) Kloosterboer, J. G.; Lijten, G. F. C. M.; Zegers, C. P. G. *Polym. Mater. Sci. Eng. Proc.* **1989**, *60*, 122−126.
(14) Kloosterboer, J. G. *Adv. Polym. Sci.* **1988**, *84*, 1−61.
(15) Kloosterboer, J. G.; Lijten, G. F. C. M. *Polymer* **1990**, *31*, 95−101.
(16) Bowman, C. N.; Peppas, N. A. *J. Appl. Polym. Sci.* **1991**, *42*, 2013−2018.
(17) Simon, G. P.; Allen, P. E. M.; Williams, D. R. G. *Polymer* **1991**, *32*, 2577−2587.
(18) Scranton, A. B.; Bowman, C. N.; Klier, J.; Peppas, N. A. *Polymer* **1992**, *33*, 1683−1689.
(19) Anseth, K. S.; Wang, C. M.; Bowman, C. N. *Polymer* **1994**, *35*, 3243−3250.
(20) Anseth, K. S.; Wang, C. M.; Bowman, C. N. *Macromolecules* **1994**, *27*, 650−655.
(21) Anseth, K. S.; Kline, L. M.; Walker, T. A.; Anderson, K. J.; Bowman, C. N. *Macromolecules* **1995**, *28*, 2491−2499.
(22) Anseth, K. S.; Bowman, C. N.; Peppas, N. A. *J. Polym. Sci., Polym. Chem.* **1994**, *32*, 139−147.
(23) Thakur, A.; Banthia, A. K.; Maiti, B. R. *J. Appl. Polym. Sci.* **1995**, *58*, 959−966.
(24) Odian, G. *Principles of Polymerization*, 3rd ed.; Wiley: New York, 1991; p 286.
(25) Bland, M. H.; Peppas, N. A. *Biomaterials* **1996**, *17*, 1109−1114.
(26) Whitney, R. S.; Burchard, W. *Makromol. Chem.* **1980**, *181*, 869−890.

(27) Landin, D. T.; Macosko, C. W. *Macromolecules* **1988**, *21*, 846−851.
(28) Bowman, C. N.; Peppas, N. A. *Macromolecules* **1991**, *24*, 1914−1920.
(29) Anseth, K. S.; Bowman, C. N. *Polym. React. Eng.* **1992−93**, *1*, 499−520.
(30) Kurdikar, D. L.; Peppas, N. A. *Macromolecules* **1994**, *27*, 4084−4092.
(31) Vrentas, J. S.; Duda, J. L. *J. Polym. Sci., Polym. Phys. Ed.* **1977**, *15*, 403−416.
(32) Vrentas, J. S.; Duda, J. L. *J. Polym. Sci., Polym. Phys. Ed.* **1977**, *15*, 417−439.
(33) Rice, S. In *Diffusion-Limited Reactions*; Bamford, C. H., Tipper, C, F. H., Compton, R. G., Eds.; Elsevier: New York, 1985; p 3.
(34) McCurdy, K. G.; Laidler, K. J. *Can. J. Chem.* **1964**, *42*, 818−824.
(35) Kurdikar, D. L.; Peppas, N. A. *Macromolecules* **1994**, *27*, 733−738.
(36) Vrentas, J. S.; Vrentas, C. M. *J. Appl. Polym. Sci.* **1991**, *42*, 1931−1937.
(37) Zielinski, J. M.; Duda, J. L. *AIChE J.* **1992**, *38*, 405−415.

MA9806110